Growth and Characterization of Germanium-Based Type I Clathrate Thin Films Deposited by Pulsed Laser Ablation

Journal:	*30th International Conference on Advanced Ceramics and Composites*
Manuscript ID:	ICACC-0175-2007.R1
Symposium:	S6
Date Submitted by the Author:	n/a
Complete List of Authors:	Hyde, Robert; University of South Florida, Physics
Keywords:	thin films, lasers, deposition, thermoelectric properties

GROWTH AND CHARACTERIZATION OF GERMANIUM-BASED TYPE I CLATHRATE THIN FILMS DEPOSITED BY PULSED LASER ABLATION

Robert Hyde, Matt Beekman, George S. Nolas, Pritish Mukherjee, and Sarath Witanachchi
Laboratory for Advanced Material Science and Technology (LAMSAT), Department of Physics, University of South Florida
4202 East Fowler Avenue
Tampa, Florida 33620

ASTRACT

Thin films of type I clathrate material, $Ba_8Ga_{16}Ge_{30,}$ have been grown using the pulsed laser ablation technique. These materials hold the potential for thermoelectric applications. Films have been deposited on a variety of substrates including silicon, quartz, sapphire, glass substrates, and YSZ cubic zirconium. Optimal crystalline films were obtained at a growth temperature of 400^{o}C and laser fluences at 3 J/cm^2 and above. The optimum laser fluence to produce stoichiometric films with the lowest particle density has been determined. The low ablation threshold for the UV wavelength leads to the particulate ejection during laser-target interaction. Excitation of the UV laser generated plasma by a second pulsed IR laser further reduced particulates and produced broader expansion profiles leading to large area uniform films.

INTRODUCTION

The thermoelectric effect, or Peltier–Seebeck effect, is the conversion of temperature differentials to electric voltage and vice versa [1]. As Seebeck observed in 1821, when a thermal gradient is maintained along the length of a material, a thermoelectric field that is proportional to the temperature gradient is induced. The electric potential produced by a temperature difference is known as the Seebeck effect and the proportionality constant is called the Seebeck coefficient (S) where $S = \Delta V/\Delta T$ and is governed by the intrinsic properties of the material. Thermoelectrics are based on the 1834 discovery of the Peltier effect, by which DC current applied across two dissimilar materials causes a temperature differential. The Seebeck effect acts on a single conductor, whereas the Peltier effect is a typical junction phenomenon [2].

In a thermoelectric material there are free carriers which carry both charge and heat. If a temperature gradient exists along a thermoelectric material, where one end is cold and the other is hot, the carriers at the hot end will move faster than those at the cold end. The faster hot carriers will diffuse further than the cold carriers and so there will be a net build up of carriers (higher density) at the cold end. The density gradient will cause the carriers to diffuse back to the hot end. In the steady state, the effect of the density gradient will exactly counteract the effect of the temperature gradient so there is no net flow of carriers. The buildup of charge at the cold end will also produce a repulsive electrostatic force (and therefore electric potential) to push the charges back to the hot end. If the free charges are positive (the material is p-type), positive charge will build up on the cold end which will have a positive potential (ΔV_p). Similarly, negative free charges (n-type material) will produce a negative potential at the cold end (ΔV_n) [3]. Therefore, a p-type and an n-type semiconductor can be connected to form an electrical series by thermally parallel device that would have a net potential difference of $|\Delta V_p| + |\Delta V_n|$. The Seebeck coefficient is very low for metals, being a few μV/K, while it is greater than 100 μV/K for semiconductors. A typical arrangement of a power-generation module is shown in Figure 1.

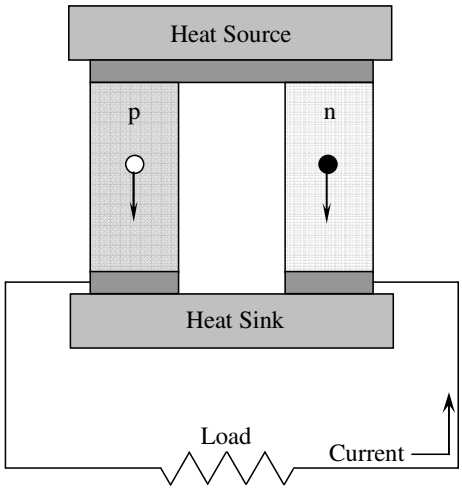

Figure 1. Typical thermoelectric device for power generation.

In order to convert thermal power into electrical power (*IV*) the following properties are desirable for the material; (a) low thermal conductivity, κ, to maintain the temperature gradient, (b) relatively high electrical conductivity, σ, to support a high current, and (c) a high voltage drop across the material per unit temperature, which is the Seebeck coefficient *S*. The combination of these requirements for a high efficiency thermoelectric device is represented by the figure-of-merit parameter (*ZT*) defined as $ZT = S^2\sigma T/\kappa$. Since metals and insulators have low values of σ/κ, good candidates for high *ZT* values are narrow band gap semiconductors [4].

Thermoelectric materials research over the last 30 years has obtained a figure-of-merit (*ZT*) of about 1. If a material system with a dual character can be constructed, where it behaves like a phonon glass towards thermal phonons to scatter them while behaving like a defect-free crystal towards electrons to maximize the electrical conduction, a so-called "phonon-glass electron-crystal" (PGEC) [5, 6]. With this, the research in thermoelectric materials is heading toward the discovery of an optimized PGEC material system where *ZT* values of 4 are possible [7]. The class of materials known as clathrates fulfills many of the PGEC requirements [8] and it was shown that these materials include potential candidates for thermoelectric applications, by Nolas *et al.* [9].

Clathrate compounds comprise a class of materials in which frameworks encapsulate loosely bonded atoms or molecules, commonly referred to as 'guests'. The type I clathrate structure is characterized by a framework typically composed of Group IV elements, which occupy sites at the vertices of face-sharing polyhedra, six tetrakaidecahedron and two pentagonal dodecahedron per cubic unit cell. Guest atoms in turn occupy the crystallographic sites found inside these polyhedra, and a general chemical formula for type I clathrates can be written as $A_8X_yY_{46-y}$, where A represents the guest atom, and X and Y represent the Group IV or substituting framework atoms [10]. The framework polyhedra that forms the type I clathrate structure is shown in Figure 2.

Type I clathrates show promising thermoelectric properties [9]. Some type I clathrates such as $Sr_8Ga_{16}Ge_{30}$ possess very low thermal conductivities, with temperature dependences similar to those of amorphous SiO_2 [7,11]. This has been explained by the unique interaction of the host framework heat-carrying phonons with the localized vibrational modes of the guests which may scatter these phonons [7, 12]. The loosely bound guests in these crystalline materials

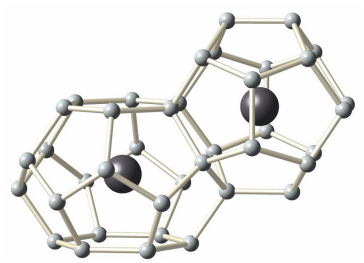

(a)

Figure 2. The framework polyhedra that forms the type I clathrate structure. The framework atoms are shown in light grey, while the guest atoms are shown in dark grey.

can undergo large, localized low-frequency vibrations, which can scatter the heat-carrying acoustic phonons resulting in thermal conductivities with magnitudes similar to amorphous materials. The low thermal conductivity combined with the relatively high power factors reported at high temperature for clathrates such as $Ba_8Ga_{16}Ge_{30}$ [13] are why these materials continue to be actively investigated in the field of thermoelectrics. The clathrate guest-host interaction continues to be of scientific interest and as a result of the interesting properties and technological promise of type I clathrates, bulk properties of these materials have been studied extensively using a wide range of experimental and theoretical techniques. However, to date no reports exist on the production and characterization of type I clathrate thin films [14]. In this paper we report the first results on the growth and structural characterization of germanium-based clathrate thin films of $Ba_8Ga_{16}Ge_{30}$ using pulsed laser deposition. One of the main advantages of laser ablation for thin film growth is the ability of this process to closely reproduce the target stoichiometry in the deposited film [15-17]. Therefore, laser ablation is uniquely suited for the growth of multi-component films from a single composite target such as $Ba_8Ga_{16}Ge_{30}$.

EXPERIMENTAL DETAILS

Type I clathrates used for laser ablation targets were prepared by mixing stoichiometric quantities of the high purity elements Ba (99%, Aldrich), Ga (99.9999%, Chameleon), and Ge (99.99%, Alfa Aesar). The mixtures were placed in pyrolytic boron nitride crucibles, and sealed in fused quartz ampoules under high purity nitrogen gas at a pressure of 2/3 atmosphere. The mixtures were heated at 1^oC/min to form $Ba_8Ga_{16}Ge_{30}$, held at 1000^oC for 24 hours, and then cooled at a rate of 2^oC/min. Targets for ablation were produce by hot and cold pressing procedures to a compacted density of higher than 95% of the theoretical X-ray density, as analyzed by powder X-ray diffraction (XRD) [14].

The pulsed laser ablation system used for single laser and dual laser ablation film growth is shown in Figure 3. In the single laser ablation process excimer laser pulses with a wavelength of 248 nm and duration of 25 ns are focused onto the rotating target placed in a 10^{-7} torr vacuum. The laser-target interaction generates a plasma plume of the target species that expands into the vacuum. The plume is allowed to deposit on a heated substrate placed on-axis 6 cm from the target. For dual-laser ablation, a CO_2 laser with pulse duration of 250 ns and wavelength of 10.06 μm was focused to spatially and temporally overlap the excimer laser spot on the target surface. The delay between the two lasers was monitored and adjusted to obtain the minimum particulate generation. Reported films of $Ba_8Ga_{16}Ge_{30}$ were deposited on quartz substrates from room temperature to 600^oC to an on-axis thickness of 6000 Å. The stoichiometry was studied by energy dispersive spectroscopy (EDS) analysis, the crystal structure characterization of the films

was performed by X-ray diffraction (XRD) analysis, and the surface morphologies of the films were investigated by scanning electron microscopy (SEM).

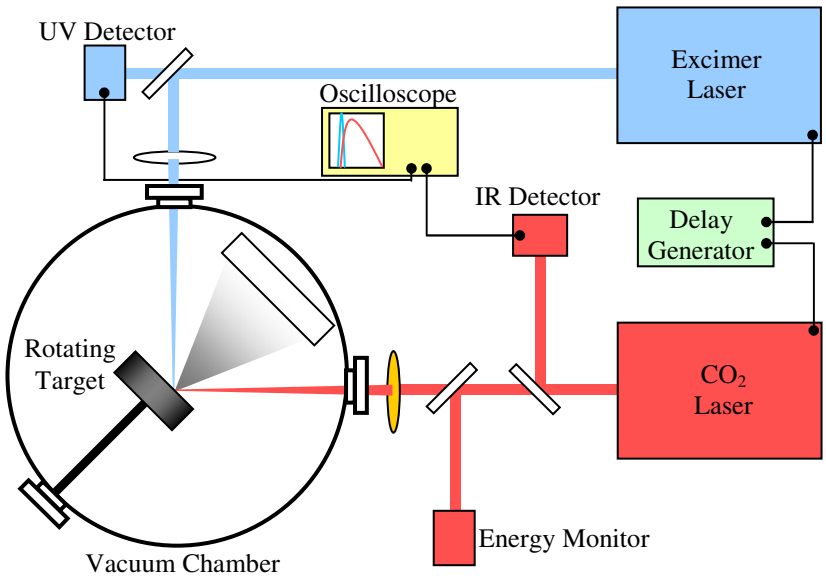

Figure 3. Diagram of the laser ablation system.

RESULTS AND DISCUSSION

The on-axis film deposition rate per laser pulse as a function of the single excimer laser fluence is shown in Figure 4. The cut-off fluence is approximately 0.5 J/cm^2 below which no detectable deposition occurs. At low laser fluences the ion density and the energy of the evaporated species as well as the rate of film growth is significantly low.

The elemental ratios of the films obtained by EDS analysis were similar for single laser

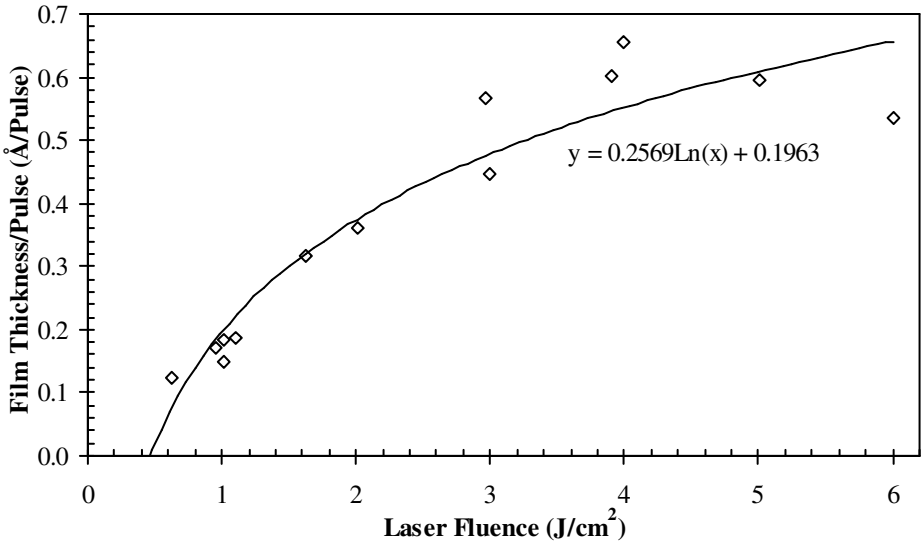

Figure 4. On-axis film deposition rate as a function of the incident single laser fluence.

ablation fluences in the range of 1 to 6 J/cm^2 and maintained the approximate stoichiometry of the target of $Ba_8Ga_{16}Ge_{30,}$ as shown in Figure 5. However, the stoichiometries deviated at laser fluences lower than 1 J/cm^2.

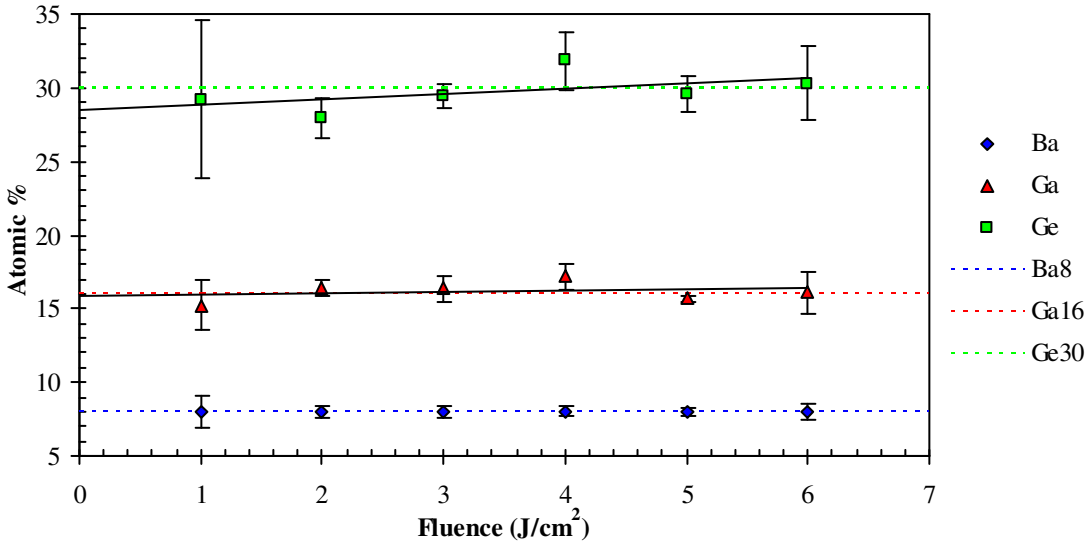

Figure 5. EDS atomic percent analysis of thin films as a function of the incident laser fluence.

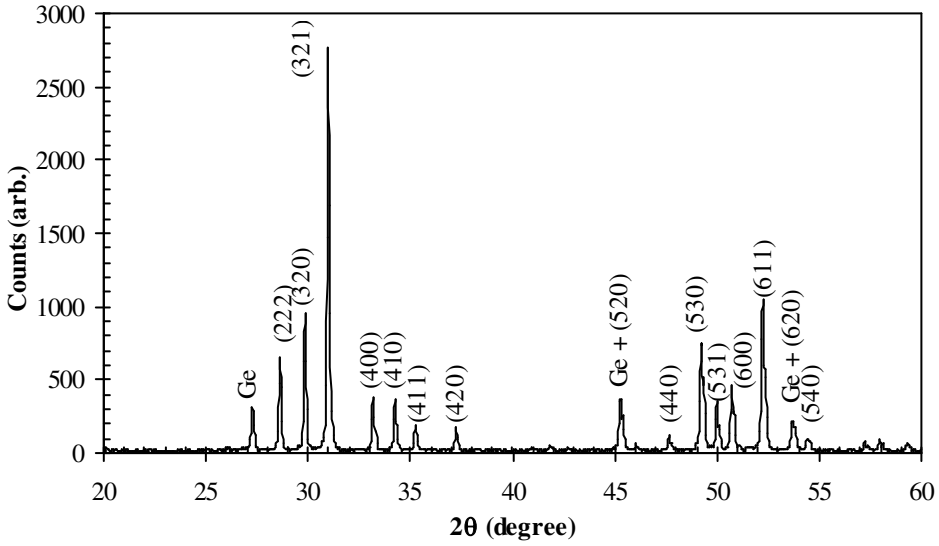

Figure 6. X-ray diffraction pattern of the $Ba_8Ga_{16}Ge_{30}$ target used for laser ablation.

Crystallinity of the films was determined by X-ray diffraction. The X-ray diffraction peaks produced by the target is shown in Figure 6. Figure 7 shows the x-ray diffraction patterns for films deposited in the temperature range of room temperature to 500 °C. The clathrate peak corresponding to the (321) orientation is clearly seen. A maximum intensity of the peak appearing at 2Θ equal to 31.2° (321) occurs at a substrate temperature of 400°C, as shown in Figure 8. Figure 9 shows the x-ray diffraction patterns for films deposited at a substrate temperature of 400 °C in the laser fluence range of 1 to 6 J/cm^2 as compared to the target pattern.

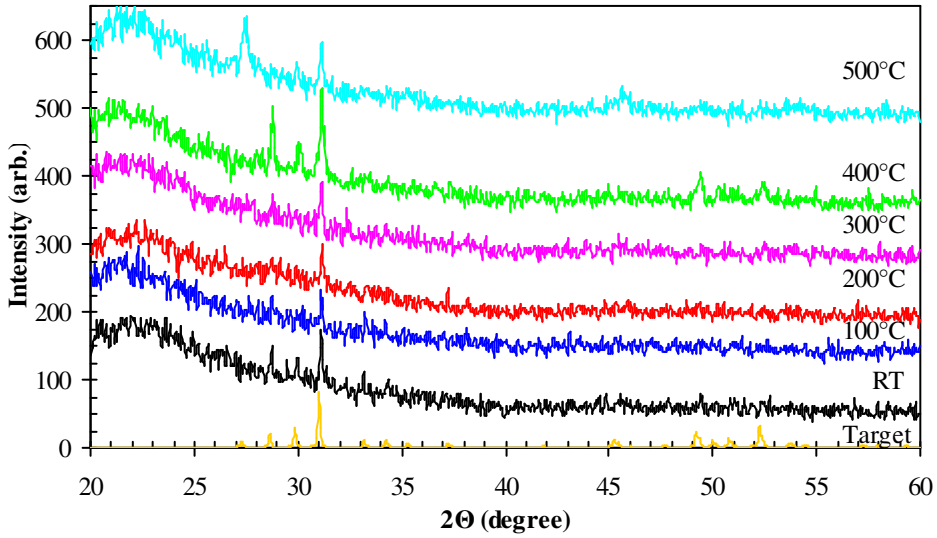

Figure 7. X-ray diffraction patterns of clathrate films on quartz substrates at temperatures from room temperature to 500°C.

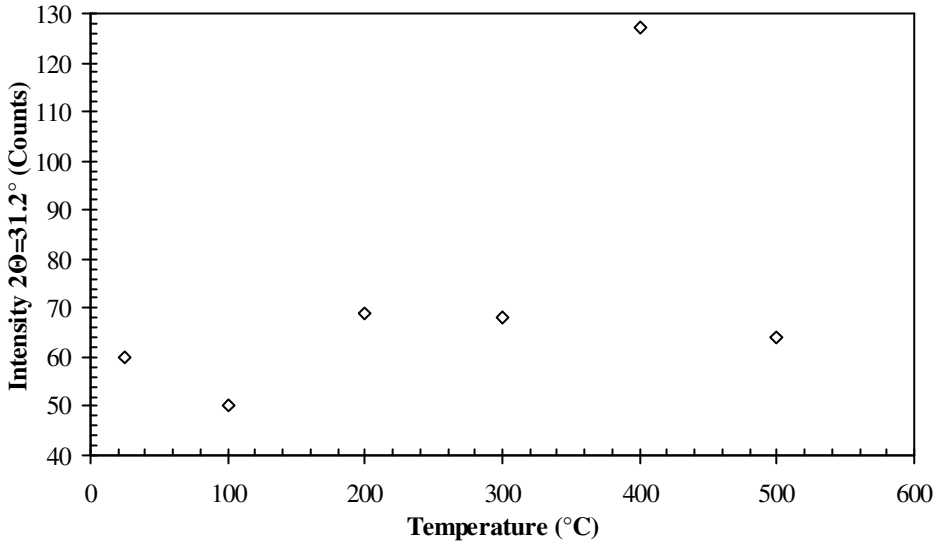

Figure 8. XRD intensity of peak 31.2 ° (321) as a function of temperature.

The intensity of the peak appearing at 2Θ equal to 31.2° (321) at the various laser fluences is shown in Figure 10. The intensity rises to a maximum and plateaus at approximately 3 J/cm^2.

With increasing laser fluence the ion density of the plasma increases leading to enhanced absorption of the laser radiation into the plasma. This increases the plasma temperature that causes the particulates in the plasma to re-evaporate. However, for very high fluences density of particles ejected increases as well. The surface morphology of $Ba_8Ga_{16}Ge_{30}$ films deposited with laser fluences from 1 J/cm^2 to 4.0 J/cm^2 have been studied by SEM. Particulate density was relatively high for both low and high fluences, as shown in Figure 11. Large molten droplets occur at higher laser fluences as is problematic with metallic sources. If the molten zone of the laser-target spot is further heated by pumping it with a CO_2 laser pulse, further reduction in particulate ejection can be expected. Figure 12 shows an example of the oscilloscope traces of

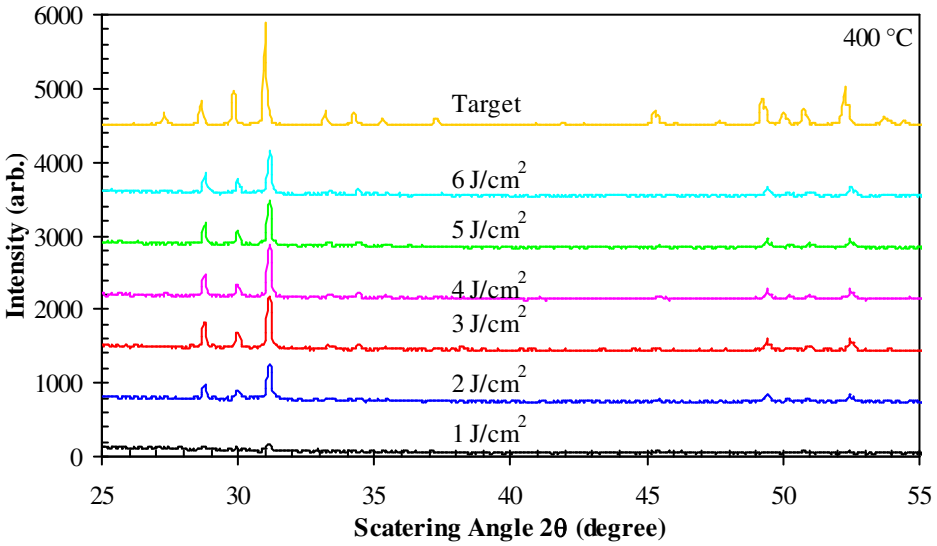

Figure 9. X-ray diffraction patterns of the clathrate films at laser fluences in the range of 1 to 6 J/cm^2.

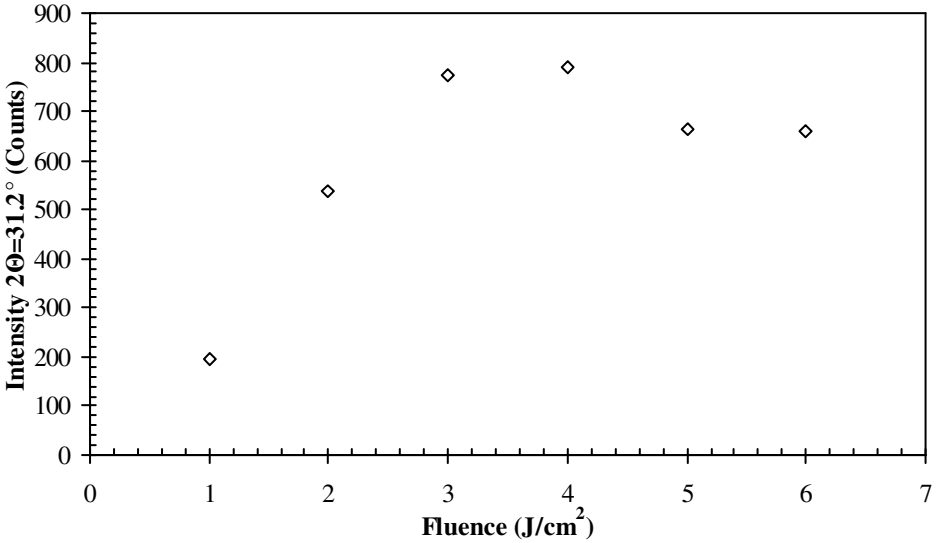

Figure 10. XRD intensity of peak 31.2 ° (321) as a function of laser fluence.

the laser pulse timing between the UV excimer laser and the IR CO_2 laser at a peak-to-peak delay of 100 ns (-22 ns from the onset of the CO_2 laser pulse to the onset of the excimer laser pulse) where the IR pulse arrives slightly before the excimer pulse. Figure 13 shows SEM images of a single laser ablated film and three films utilizing the dual laser technique at various laser delays; 146 ns peak-to-peak (2 ns from onset), 100 ns peak-to-peak (-22 ns from onset), and -23 ns peak-to-peak (-140 ns from onset). The excimer laser was operated at a fluence of 1 J/cm^2 and the CO_2 laser at a fluence of 0.4 J/cm^2. The minimum particulate generation was observed while using a 100 ns delay. As seen in Figure 13(c) that the majority of the large particles have been eliminated by maintaining a melt-zone on the target surface produced by the dual laser process. Optimization of the technique is being investigated to further reduce the particulates.

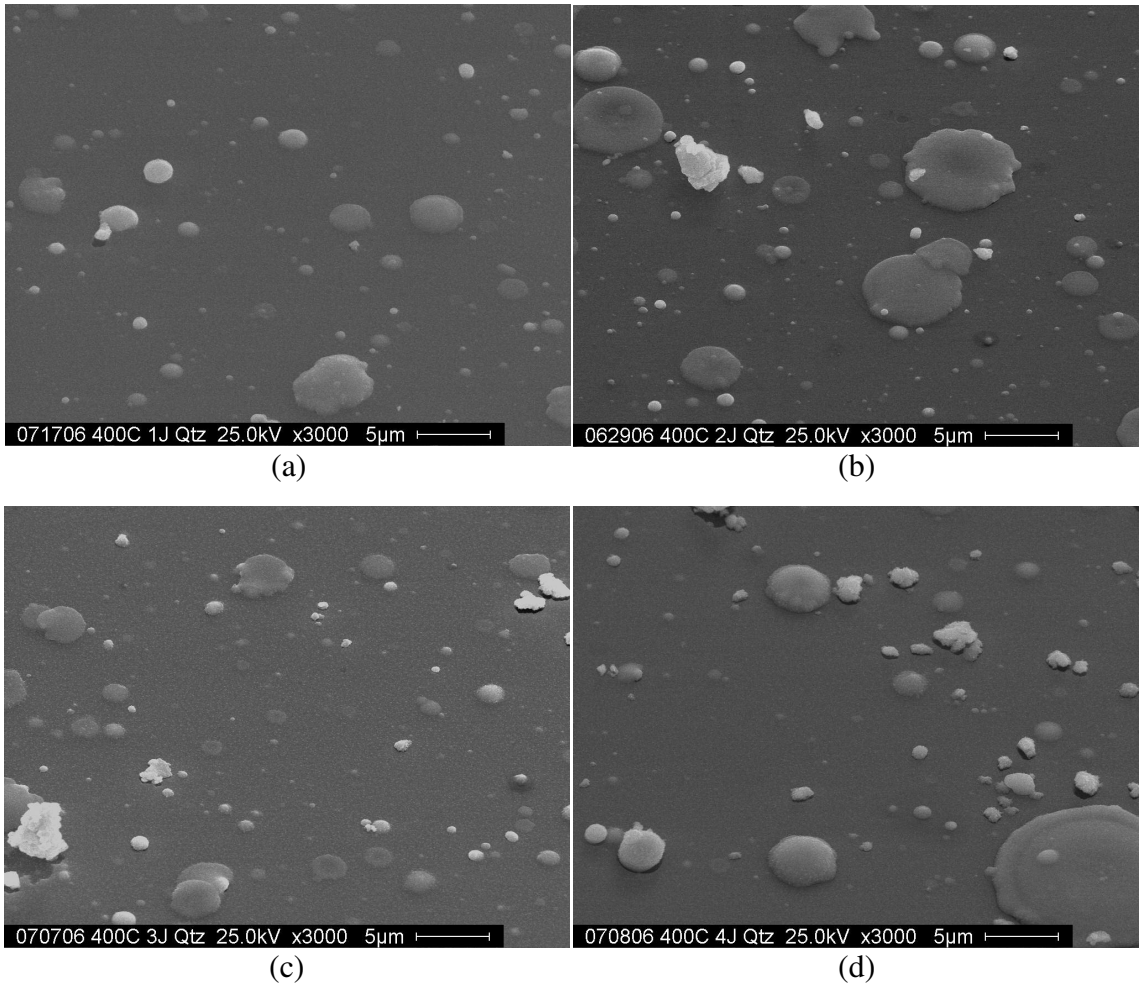

Figure 11. SEM images of clathrate films deposited with single laser ablation fluences of (a) 1 J/cm^2 (b) 2 J/cm^2 (c) 3 J/cm^2 and (d) 4 J/cm^2.

SUMMARY

We have successfully demonstrated the use of pulsed laser ablation techniques for the stoichiometric growth of crystalline thin films of the type I clathrate $Ba_8Ga_{16}Ge_{30}$. The ablation threshold for the material at UV wavelengths appears to be low, approximately 0.5 J/cm^2. Stoichiometry of the films deposited near this threshold deviated from the required 8:16:30 ratio. Partial evaporation of the species at the target at low laser fluences may be responsible for this effect. However, for laser fluences above 1 J/cm^2 films retained the proper stoichiometry. With increasing fluence the density of particles deposited on the film also increased. We have utilized a dual-laser approach by coupling the energy of a CO_2 laser into the laser-target molten-zone at the optimum inter-pulse delay to minimize the ejection of particulates from the target. The experiments showed that for optimum delay between the onset of the excimer and CO_2 laser pulses to produce films with low particle density is approximately 22 ns (100 ns peak-to-peak).

ACKNOWLEDGEMENTS

This project is partially supported by the US Department of Energy, under Grant No. DE-FG02-04ER46145 and by the National Science Foundation, under Grant No. DMI-0217939.

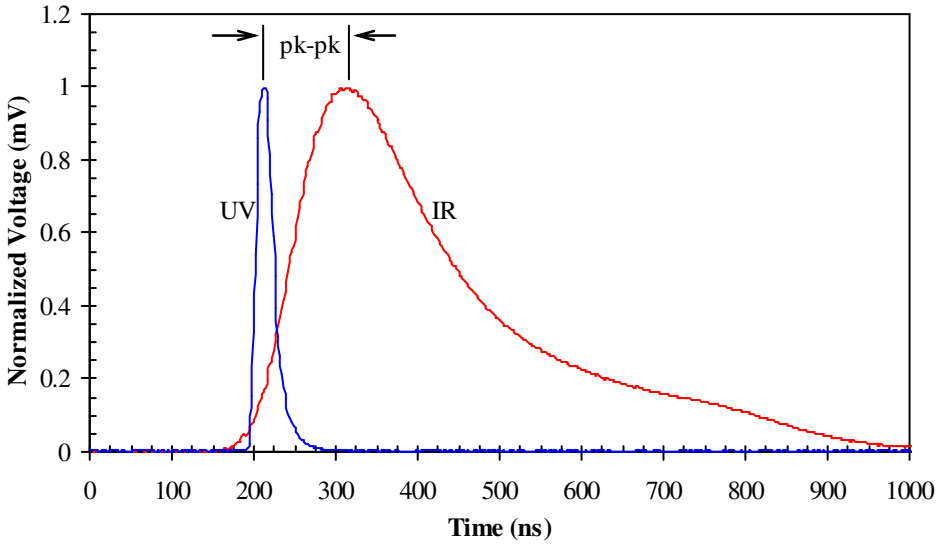

Figure 12. An example of oscilloscope traces of the excimer pulse (UV) and the CO_2 laser pulse (IR) with a 100 ns peak-to-peak delay.

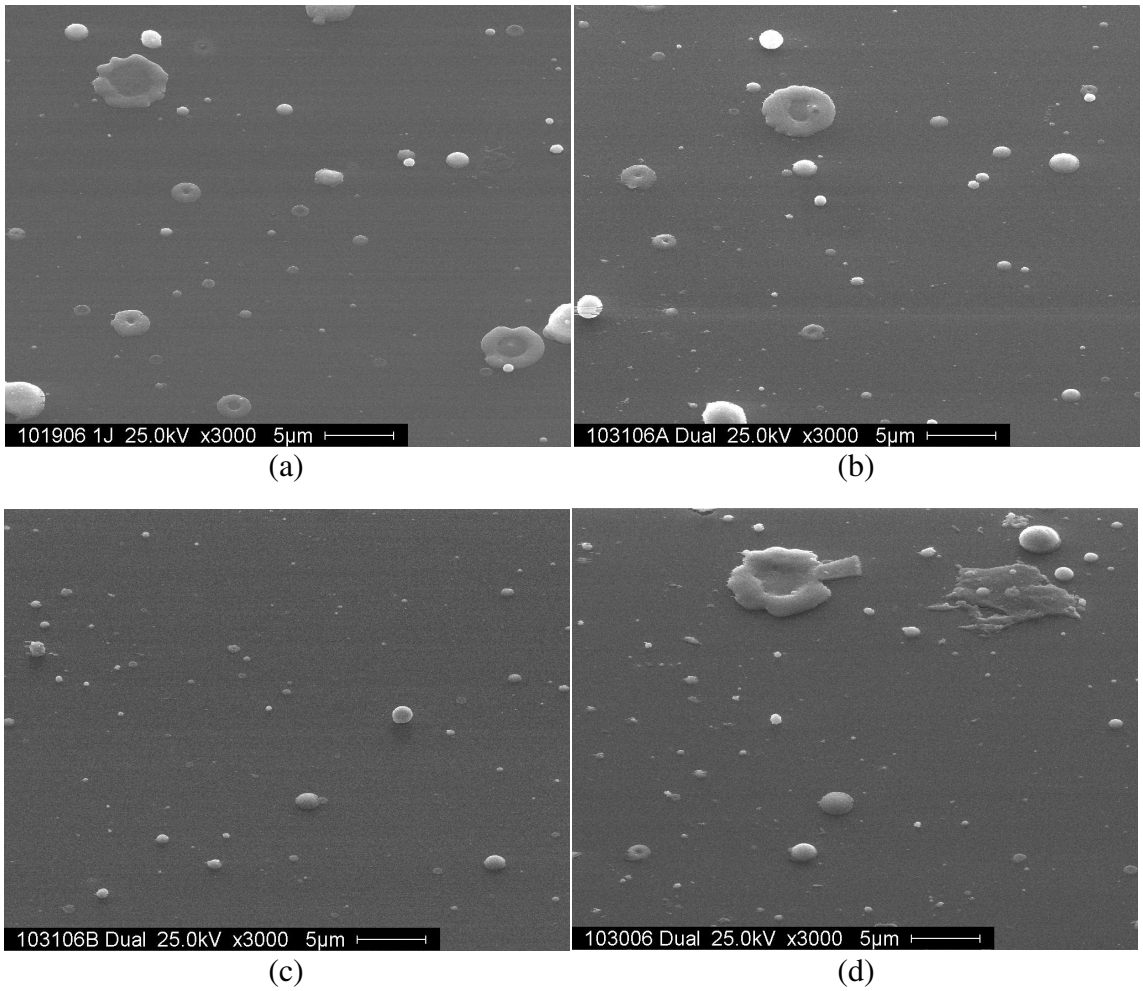

Figure 13. SEM images of clathrate films deposited with (a) 1 J/cm^2 single laser fluence and dual laser peak-to-peak delays of (b) 146 ns (c) 100 ns and (d) -23 ns.

REFERENCES

[1] R. M. Besançon (1985). *The Encyclopedia of Physics, Third Edition*. Van Nostrand Reinhold Co. (1985).
[2] Melcor Corp., *Thermoelectric Handbook*, Sept., (1995).
[3] *CRC Handbook of Thermoelectrics, Introduction*, D.M. Rowe (ed.), CRC Press, (1995).
[4] G. S. Nolas, G. A. Slack, and S. B. Schujman. "Semiconductor Clathrates: A Phonon-Glass Electron-Crystal Material with Potential for Thermoelectric Applications" in *Recent Trends in Thermoelectric Materials Research I*, T. M. Tritt (ed.) *Semiconductors and Semimentals* V. 69 (Academic Press 2000).
[5] T. M. Tritt (ed.) *Semiconductors and Semimetals* V. 69, 70, and 71 (Academic Press, 2001)
[6] G. A. Slack "New Materials and Performance Limits for Thermoelectric Cooling" CRC Handbook of Thermoelectrics, ed. D. M. Rowe 407-440 (CRC Press. 1995).
[7] J. P. Heremans, C. M. Thrush, and D. T. Morelli, "Thermopower Enhancement in Lead Telluride Nanostructures", Phys. Rev. B 70, 115334 (2004).
[8] G. A. Slack, Mater. Res. Soc. Symp. Proc. **478** 47 (1997).
[9] G. S. Nolas, J. L. Cohn G. A. Slack, and S. B. Schujman. Appl.Phys. Lett. 73. 187 (1998).
[10] G. S. Nolas, G. A. Slack, and S. B. Schujman. "Semiconductor Clathrates: A Phonon-Glass Electron-Crystal Material with Potential for Thermoelectric Applications" in *Recent Trends in Thermoelectric Materials Research I*, T. M. Tritt (ed.) *Semiconductors and Semimentals* V. 69 (Academic Press 2000).
[11] J. L. Cohn G. S. Nolas, V. Fessatidis, T. H. Metcalf, and G. A. Slack. Phys. Rev. Lett. **82.** 779 (1999).
[12] Nolas, G.S., Weakley, T.J.R., Cohn, J.L., and Sharma, R., "Structural properties and thermal conductivity of crystalline clathrates," *Phys. Rev. B* **61**, 3845 (2000).
[13] Saramat, A. et al., "Large thermoelectric figure of merit at high temperature in Czochralski-grown clathrate $Ba_8Ga_{16}Ge_{30}$," *J. Appl. Phys.* **99**, 023708 (2006).
[14] S. Witanachchi, R. Hyde, H. S. Nagaraja, M. Beekman, G. S. Nolas, and P. Mukherjee, "Growth and Characterization of Germanium-based Type I Clathrate Thin Films Deposited by Pulsed Laser Ablation" Mater. Res. Soc. Symp. Proc. Vol. 886 Materials Research Society 401-406 (2006).
[15] Witanachchi, S., Ahmed, K., Sakthivel, P., and Mukherjee, P., "Dual-laser ablation for particulate-free film growth *Appl. Phys. Lett.* 66, 1469 (1995).
[16] Mukherjee, P., Cuff, J.B., and Witanachchi, S., "Plume expansion and stoichiometry in the growth of multi-component thin films using dual-laser ablation," *Appl. Surface Sci.* **127-129**, 620 (1998).
[17] Mukherjee, P., Chen, S., Cuff, J.B., Sakthivel, P., Witanachchi, S., "Evidence for the physical basis and universality of the elimination of particulates using dual-laser ablation. I. Dynamic time-resolved target melt studies, and film growth of Y2O3 and ZnO," *J. Appl. Phys.* **91**, 1828 (2002).